Analysis of Spring-Back Behaviour in Sheet Metal U-Bending Using Finite Element Methods

Tarun Nharwal
Research Scholar, Mangalayatan University (MU), Aligarh, Uttar Pradesh, India.

Abstract

This study investigates the spring-back characteristics in the sheet metal U-bending process using finite element analysis. The elastic recovery phenomenon, known as spring-back, poses significant challenges in ensuring dimensional accuracy in sheet metal forming. The study employs an updated Lagrangian thermo-elastoplastic finite element method to analyze the effects of various process parameters on spring-back. Key findings demonstrate that the punch corner radius, punch-die clearance, and friction coefficient are major influencers, while the punch velocity and sheet thickness have minimal impact. This research provides insights for tool designers to enhance prediction accuracy and suppress elastic recovery.
Keywords: spring-back characteristics; Finite element analysis; sheet metal U-bending process; punch corner radius.

INTRODUCTION

Sheet metal forming is a widely used technique in nearly all industrial sectors due to its efficiency in producing final sheet products with the desired shape and appearance using relatively simple tools. However, challenges such as wrinkles, tears, and poor dimensional precision often arise if tool and process parameters are not carefully controlled. A critical issue in the sheet metal bending process is the elastic recovery after unloading, known as spring-back, which leads to dimensional inaccuracies and sidewall curl [1]. Therefore, designing tools that account for the material and final product dimensions requires accurate predictions of spring-back.

Traditionally, process parameter identification has relied heavily on trial-and-error, drawing on the designer's empirical knowledge or time-consuming, costly trials. Elastic recovery is influenced by several factors, including tool shape, material properties, temperature fluctuations, and frictional contact conditions [2, 3]. The nonlinear nature of these interactions complicates mathematical modeling, limiting the accuracy of traditional prediction methods [4, 5].

Recent advancements in numerical simulations, particularly the finite element method (FEM) and numerical optimization, have significantly improved the precision of spring-back predictions, enabling more systematic tool design. Sheet metal bending, as an out-of-plane forming process, involves minimal strain but considerable deformation, further complicated by changing frictional boundaries and an interdependent temperature field during the process. As a result, finite element analysis of the bending process remains a complex challenge that continues to drive research efforts [6–8].

This study addresses a gap in the understanding of how key process parameters affect elastic recovery, focusing specifically on the spring-back phenomenon. Using a thermo-elastoplastic finite element approach integrated with the updated Lagrangian framework, this research simulates plane-strain sheet metal U-bending to investigate the parametric dependence of spring-back [9]. The methodology and finite element approximation used in the study are detailed in the subsequent sections.

The issue of spring-back in sheet metal forming has been the subject of extensive study. Bian and Li (2024) [10] provided critical insights by using the updated Lagrangian framework to model elastic recovery under varied process conditions. However, Sarath and Paul (2021) [11] highlighted that theoretical models face challenges in accurately predicting spring-back due to nonlinearities in material behaviour, tool geometry, and thermal fields. Recent advancements in computational techniques, especially the finite element method (FEM), have significantly improved the ability to simulate and predict

Email ✉: tarunnharwal@aol.com

these complex processes. For instance, the work of Chisena, Chen, and Shih (2021) [12] demonstrated how FEM advances allow for more refined simulations of the factors affecting spring-back. Similarly, Hou et al. (2023) [13] emphasized that precise parameter identification and predictive modeling remain key research priorities. Recent studies in this domain are focusing on enhancing FEM methodologies to address material and process intricacies, enabling better accuracy in predicting spring-back behaviour.

In addition, modern trends in digital preservation and computational efficiency are reshaping FEM applications. The integration of cloud computing and AI-driven optimizations in numerical modeling has led to more accessible and efficient simulations. Digital preservation of data ensures that simulations and parametric studies can be archived, shared, and reused, facilitating continuous improvements and collaboration in FEM research. These technological advancements are allowing for more detailed and scalable investigations into spring-back and other deformation behaviors.

Objective of Study

The primary objective of this work is to examine the spring-back phenomenon in the sheet metal U-bending process through advanced finite element analysis.

Problem Statement

This study investigates the challenge of precisely predicting and managing the spring-back phenomenon in the U-bending process of sheet metal. Spring-back, resulting from elastic recovery post-unloading, induces dimensional errors in fabricated metal components. This issue is intricate because to the impact of several process parameters, such as tool shape, material characteristics, and friction conditions. The research aims to elucidate this complexity by finite element analysis to enhance comprehension of the effects of these characteristics and deliver dependable forecasts for tool and process design.

Sheet Metal U-Bending Process

Fig. 1(a) depicts two-dimensional schematic representation of a simple sheet metal U-bending configuration. In general, we may consider a whole U-bending process into two steps, loading and unloading. In the loading step, a sheet metal is being bent into the die until the punch moves down completely, so that its shape is formed closely to the die shape. During this step, the workpiece undergoes elastoplastic deformation and temperature increase under frictional resistance. Next, the deformed sheet metal is ejected from the tool set during the unloading step; while experiencing the residual stress release and the temperature drop to reach a thermo-mechanical equilibrium state.

Owing to this thermo-mechanical relaxation, dimension of the final product, particularly the bending angle, becomes different from that of the product before unloading. This dimensional difference is called the elastic recovery phenomenon, particularly the bending angle alternation is denoted by spring-back. The spring-back amount is defined in Fig. 1(b). In particular, the negative spring-back is also called spring-go.

In sheet metal U-bending process two sets of field equations are coupled, elastoplasticity and unsteady-state heat transfer. As is well known, the former exhibits the highly nonlinear behaviour due to material, geometry and contact boundary nonlinearities. Meanwhile, the temperature change is remarkably smaller than that in hot metal forming, but its influence on the spring-back amount is not negligible

Thermo-Elastoplastic Deformation

The material model for elastoplastic materials with strainhardening can be defined in different ways, but we in this paper use the following form:

Strain-hardening yielding: $\bar{\sigma}\left(\sigma_Y, \bar{\varepsilon}_p\right) = \sigma_Y + K\left(\bar{\varepsilon}_p\right)^m$........(1.1)

Effective plastic strain : $\bar{\varepsilon}_p = \bar{\varepsilon} - \bar{\varepsilon}_0$........(1.2)

In which the effective stress $\bar{\sigma}$ is defined by $\sqrt{3/2}\left(s_{ij}s_{ij}\right)^{1/2}$ with the deviatoric stresses s_{ij}, and the effective strain $\bar{\varepsilon}$ is defined by $\sqrt{2/3}\left(\varepsilon_{ij}\varepsilon_{ij}\right)^{1/2}$. On the other hand, K and m denote material-dependent constants, σ_Y the initial yield stress, and $\bar{\varepsilon}_0 (= \sigma_Y/E)$ the effective strain at the initial yielding. We next need the constitutive relation between stress and strain rates for the updated Lagrangian kinematic description adopted in this study.
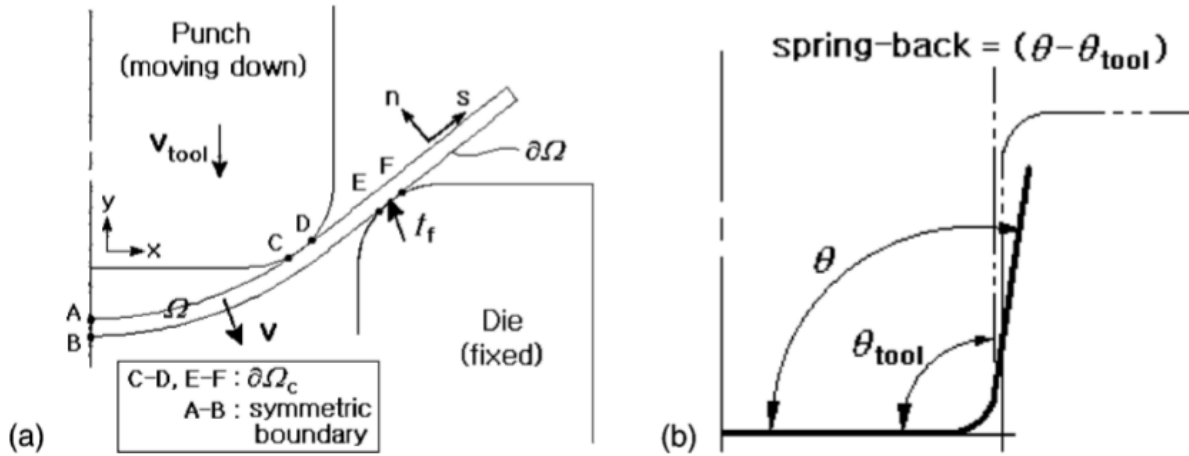

Fig. 1. Sheet metal U-bending: (a) two-dimensional schematic representation; (b) definition of spring-back

In such description, the use of the second Piola-Kirchhoff stress tensor and the Green strain tensor is general, as is well-explained in[**14, 15**]. According to the small strain deformation of sheet metal U-bending, the Jaumann (or Jaumann-Zaremba) time derivative of the Kirchhoff stress $\dot{\tau}_{ij}$ leads to the strain rate independent constitutive relation that keeps the objectivity.

Unsteady-State Heat Conduction

On the other hand, the process generates heat according to the relative frictional motion and the plastic deformation, even without any external heat supply. Since the convection and radiation effects are considerably smaller than the heat conduction, we exclude such effects in the heat transfer analysis. But the reader may refer to [**16**] for the numerical formulation of general heat transfer problems.

The unsteady-state temperature field $T(x; t)$ in the material domain Ω, during the process time $[0, t^*]$ under consideration, is expressed as follows:

$$\rho c \frac{\partial T}{\partial t} - \nabla \cdot (\kappa \nabla T) = \frac{\partial q}{\partial t} \quad \text{in } \Omega \times (0, t^*]. \ldots \ldots .. (1.3)$$

In the above problem, the internal heat generation due to the plastic deformation is calculated from the conservation of plastic work (with the heat generation efficiency e_g of 0.9),

$$\frac{\partial q}{\partial t} = e_g \sigma_{ij} \dot{\varepsilon}_{ij}. \ldots \ldots .. (1.4)$$

Thermo-Elastoplastic Finite Element Analysis
Nonlinear Finite Element Approximations:

To address the nonlinear thermo-elastoplastic problem, we use the updated Lagrangian kinematic description, where the current configuration $\Omega^{\wedge}t$ becomes the reference frame. The virtual work principle leads to the following variational formulation:

$$\int_{\Omega^t} \left[(\dot{t}_{ij} - 2\sigma_{ik}\dot{\epsilon}_{kj})\delta\dot{\epsilon}_{ij} + \sigma_{ik}v_{j,k}\delta v_{j,i} \right] dV = \int_{\delta\Omega_c} \dot{t}_i \delta v_i ds. \dots\dots\dots(1.5)$$

Next, the velocity field is approximated using the matrix $\Phi_{,\,\text{comps}}$ composed of iso-parametric finite element basis functions and the nodal vector $\bar{v}^T = \{\bar{v}_1^k, \bar{v}_2^k, \bar{v}_3^k\}$, such that:

$$v(x) = \Phi(x) \cdot \bar{v}. \dots\dots\dots(1.6)$$

The strain rate tensor and velocity gradient vector are expressed as:

$$\dot{\epsilon}(v) = D^T \Phi\bar{v} = B\bar{v}, \; v_{j,k} = (L\bar{v})_{jk}. \dots\dots\dots(1.7)$$

Substituting the finite element approximation leads to the following nonlinear matrix equations:

$$R^t = 0: K^t\bar{v} - F^t = 0. \dots\dots\dots(1.8)$$

Where R^t is the residual force-rate vector, and the global stiffness matrix and load-rate vector are defined as:

$$K^t = \int_{\Omega^t} \left[B^T D_{cp} B + L^T SL - B^T \hat{I}\dot{\Psi} \right] dV, \; F^t = \int_{\partial\Omega_\epsilon^t} \Phi^T \dot{t} ds. \dots\dots\dots(1.9)$$

The temperature field rate $\dot{T}(x)$ is approximated using the same iso-parametric basis functions:

$$\dot{T}(x) = \Psi^T(x)\dot{T}. \dots\dots\dots(1.10)$$

The heat conduction problem is formulated as:

$$\int_{\Omega^t} [\rho c\dot{T}Q + \kappa\nabla T \cdot \nabla Q]dV + \int_{\partial\Omega_c^*} h_c TQds = \int_{\Omega^t} e_g(\sigma_{ij}\dot{\epsilon}_{ij})Qds + \int_{\partial\Omega_c'} (q_f + h_c T_{\text{tool}})Qds. \dots\dots\dots(1.11)$$

For temporal discretization, we divide the time interval into steps Δt, and use the Crank-Nicolson scheme:

$$\left[C^t + \frac{1}{2}(\Delta t)K^t \right] \bar{T}^{(k+1)} = \left[C^t - \frac{1}{2}(\Delta t)K^t \right] \bar{T}^k + \Delta t F_{k+1/2}^t. \dots\dots\dots(1.12)$$

Where:

$$[C^t] = \int_{\Omega^t} \rho c\Psi^T\Psi dV, \; [K^t] = \int_{\Omega^t} \kappa\nabla\Psi \cdot \nabla\Psi dV + \int_{BR_c} h_c\Psi^T\Psi ds. \dots\dots\dots(1.13)$$

Incremental Analysis

The incremental analysis uses the updated domain Ω^t at each time step $t = 0, t + \Delta t, t + 2\Delta t, ...$, starting with the undeformed domain Ω^0. The displacement increment is defined as $\Delta \bar{u} = \bar{v}\Delta t$, and the residual equation is:

$$\Delta R^k = 0: \ K^k \Delta \bar{u}^{(k+1)} - \Delta F^k = 0. \dots \dots (1.14)$$

The iterative solution uses the Newton-Raphson method:

$$K_T^{(k,l)} \Delta \bar{u}_l^{(k+1)} = \Delta R^{(k,l)}, \ \bar{u}_l^{(k+1)} = \bar{u}_{l-1}^{(k+1)} + \Delta \bar{u}_l^{(k=1)}. \dots \dots (1.15)$$

Convergence is achieved when:

$$\frac{\left\| \delta \bar{u}_l^{(k+1)} \right\|}{\left\| \bar{u}_l^{(k+1)} \right\|} \leq \tau_U \ \text{ and } \ \frac{\left\| \delta R^{(k,l)} \right\|}{\left\| R^{(k,l)} \right\|} \leq \tau_R. \dots \dots (1.16)$$

In the unloading step, the symmetric boundary condition $u_x = 0$ is applied at the centerline, and a negative contact force $t = -f^c$ is imposed. A temperature drop $\Delta T = T_0 - T_c$ is applied, followed by steady-state linear thermo-elastic analysis

METHODOLOGY

Data Collection

The study employs a two-dimensional symmetric finite element model to conduct numerical experiments. The model parameters are defined in Figure 2(a), where key geometric factors of the workpiece and tools are outlined. The workpiece is modeled in a plane-strain state, while the tool components are treated as rigid bodies. Since the tool components do not deform, only heat transfer analysis is required for these elements. Table 1 provides the detailed numerical data, covering six variable parameters that influence the spring-back amount.

Data Collection Methods

The finite element mesh used for the simulation consists of bilinear quadrilateral elements, ensuring accurate representation of the workpiece's deformation during the process. The mesh details are also illustrated in Figure 2(a). For the parametric investigation, six process parameters—punch and die corner radii, punch-die clearance, friction coefficient, punch velocity, and sheet thickness—were varied systematically. These parameters were chosen to explore their impact on the spring-back phenomenon in sheet metal U-bending.

Data Analysis Methods

The numerical simulations were performed using commercial DEFORM code [17], leveraging its user-interface routine for ease of parameter manipulation and analysis. The simulation model integrates heat transfer and elastoplastic deformation analysis to examine the behavior of the workpiece during bending. The study focuses on understanding the effect of each parameter on spring-back, with results analyzed using the finite element method (FEM) to provide precise predictions of elastic recovery.
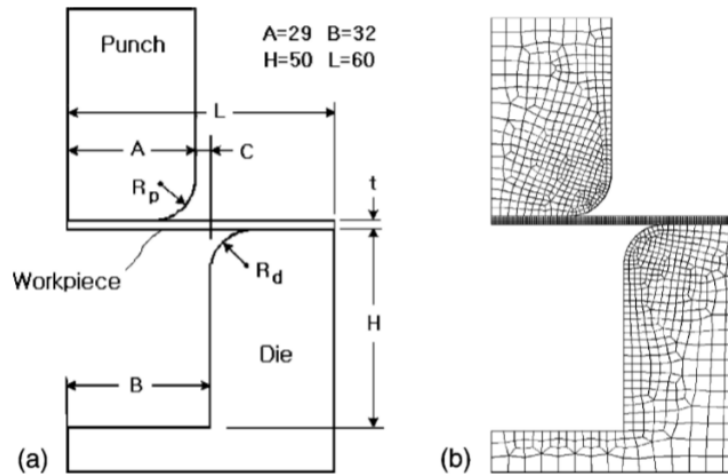
Fig. 2. Analysis model: (a) dimension definition; (b) finite element mesh

Tab. 1. Data taken for the numerical experiments

| Material data	Workpiece (Aℓ5052)	Tool (AISI H-13)
Heat capacity, ρc (N/mm² °C)	2.3584	3.5880
Conductivity, κ (N/s°C)	137.0	24.6
Yield stress, σ_Y (MPa)	195	-
Material constants, K (MPa) and m	104.33, 0.18	
Thermal expansion coefficient, α (mm/ °C)	2.57×10^{-2}	-
Conduction coefficient, h_c (N/smm °C)	11.0	
Young's modulus, E (MPa)	1×10^3	-
Poisson's ratio, v	0.33	-
Friction coefficient, μ	0.1 (variable)	
Geometry data		
Punch corner radius, R_p (mm)	10 (variable)	
Die corner radius, R_d (mm)	10 (variable)	
Punch-die clearance, C (mm)	3 (variable)	
Workpiece thickness, t (mm)	2 (variable)	
Simulation data		
Punch velocity, v_p (mm/s)	1 (variable)	
Initial time-step, Δt (s)	0.1	
Convergence tolerances, τ_U and $\tau_\Re$	0.001, 0.01	
Initial temperature, T_0 (°C)	20 (workpiece	tool)

RESULTS

The study carries out the parametric experiments investigating the effects of six parameters on the spring-back amount the punch and die corner radii, the punch–die clearance, the friction coefficient, the punch velocity and the sheet thickness. For these experiments, the specific parameter is taken variable while keeping the others as given in Table 1.

The parametric dependence of spring-back amount on the punch corner radius R_p is represented in Fig. 3(a), where the spring-back amount varies largely and almost linearly from -4° (spring-go) to +2.3° within the examination range of the punch corner radius. Compared to the effects of the other parameters, as presented next, the effect of this parameter is the

most considerable. However, the punch corner radius is directly associated with the product corner shape, so the elastic recovery control should be done together with the suitable product shape design. Fig. 3(b) shows the parametric variation of spring-back amount to the die corner radius R_d. From the detailed numerical data, the effect of die corner radius change is tiny such that the overall spring-go variation is less than 0.4° within the parameter investigation range. Furthermore, the spring-go amount becomes insensitive to the die corner radius when $R_d \geq 8$ mm. We remind that the workpiece thickness at the corner is compressed by punch load when the die corner radius becomes larger than 12 mm. The effect of the punch–die clearance is represented in Fig. 4(a), where negative spring-back becomes relaxedalmost linearly and remarkably as the clearance increases, similar to the punch corner radius. By the way, the punch–die clearance is related to surface appearance and tear of products. Hence, the elastic recovery should be suppressed by considering such effects together. On the other hand, referring to Fig. 4(b) the friction coefficient increase relaxes negative spring-back to some extent, but it leads to the almost saturated positive spring-back when $\mu \geq 0.2$. This trend implies that the elastic recovery can be suppressed by using an appropriate lubricant.
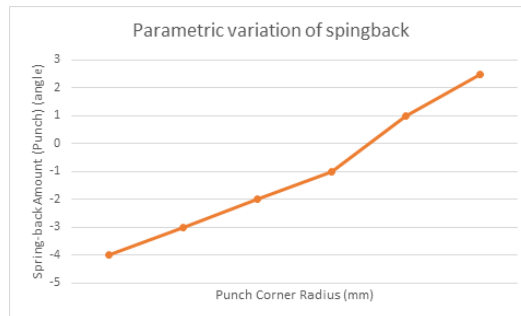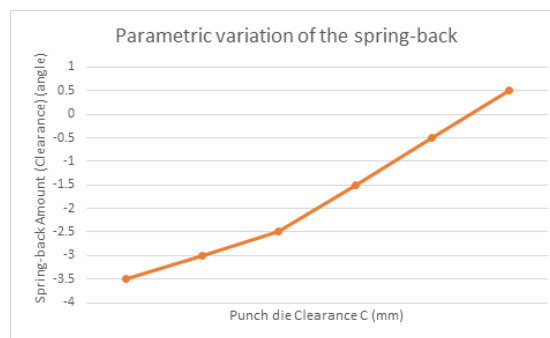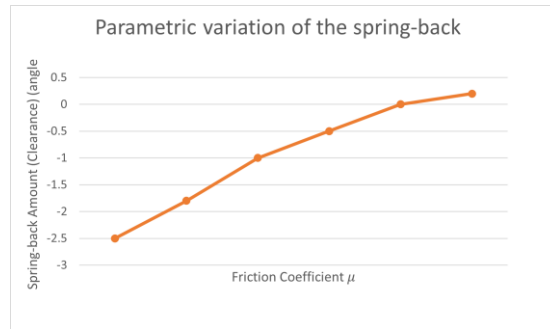

(a)
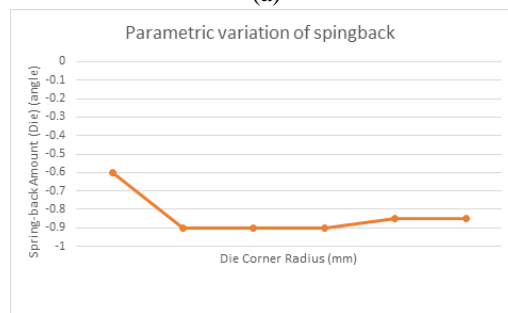
(b)

Fig. 3. Parametric variation of the spring-back amount: (a) to the punch corner radius; (b) to the die corner radius

(a)

(b)

Fig. 4. Parametric variation of the spring-back amount: (a) to the punch–die clearance; (b) to the friction coefficient.

Last two figures, Fig. 5(a) and (b), represent the springback variations with respect to the punch velocity V_p and the workpiece thickness t, respectively. Above all, both cases show the insignificant variation in the elastic recovery when compared to the previous three parameters: the punch corner radius, the punch-die clearance and the friction coefficient. If we insist on estimating, the smallest spring-back amount, for our model process, is produced with the punch velocity near V_p=5 mm/s and the workpiece thickness near either t=1.5 or 2.75 mm. However, both cases exhibit the remarkable inconsistency in the spring-back variation, and furthermore, the workpiece thickness is a primary parameter in the part design. Putting these characteristics together, both parameters are rather unsuitable in the springback suppression.

Fig. 5. Parametric variation of the spring-back amount: (a) to the punch velocity; (b) to the workpiece thickness

DISCUSSION OF RESULTS

The findings from the finite element analysis provide key insights into the spring-back behaviour during the U-bending process. One of the most significant discoveries was the impact of the punch corner radius, punch-die clearance, and friction coefficient on the spring-back magnitude. The results revealed a nearly linear increase in spring-back angle as the punch corner radius increased, indicating that sharper corners result in greater elastic recovery. This directly ties to the study's

objective of improving dimensional accuracy, suggesting that controlling the punch corner radius is critical for minimizing spring-back in tool design.

Similarly, the study found that increasing the punch-die clearance effectively reduced spring-back, emphasizing the role of tool geometry in achieving precise product dimensions. These results align with the research objective of identifying process parameters that can be optimized to control elastic recovery, suggesting that clearance adjustments offer a practical method for enhancing dimensional accuracy.

The friction coefficient also showed significant influence. An increase in friction reduced negative spring-back but reached a plateau after a certain value, indicating that while lubrication can mitigate spring-back, excessive friction may not yield further benefits. This finding strengthens the connection to the research objective by demonstrating how managing friction can optimize forming processes without unnecessary material wear or lubrication.

Conversely, the punch velocity and workpiece thickness had negligible effects on spring-back, which contrasts with prior studies that suggested otherwise. This discrepancy underscores the importance of focusing on tool geometry and frictional conditions rather than modifying velocity or thickness to control spring-back, further supporting the study's aim of identifying the most effective parameters for process improvement.

When compared to existing literature, these findings reinforce the importance of tool geometry and friction management in controlling elastic recovery, consistent with previous research. However, the results also draw attention to the overestimated role of velocity and thickness in earlier studies, suggesting a shift in focus toward more impactful variables.

While the study presents a robust framework for understanding spring-back in the U-bending process, its applicability may be limited to this specific forming method. To generalize these findings, future research should explore these parameters across various forming processes and materials, which would further extend the relevance of this work to broader manufacturing applications. Moreover, integrating more sophisticated material models into the analysis could enhance the accuracy of spring-back predictions, aligning with the broader research goal of refining predictive tools for industrial use.

CONCLUSION

This study examined the parametric variation of spring-back magnitude in plane-strain sheet metal U-bending, concerning the principal parameters related to the process. The numerical analysis was conducted using the revised Lagrangian thermo-elastoplastic finite element method using the Coulomb frictional contact model. We analysed the temperature, effective strain, effective stress distributions, and the temporal reactions of the punch load and temperature through the initial numerical experiment. The temperature fluctuation over the workpiece thickness is minimal, and the overall rise is negligible. However, the effective strain and stress demonstrate significant variation in thickness, especially in the material region adjacent to the punch corner. The parametric analysis revealed that the punch corner radius, punch-die clearance, and friction coefficient significantly influence the springback amount, whereas the remaining three factors do not. The punch corner radius and the punch-die clearance result in a nearly linear variation in the quantity of spring-back. The friction coefficient exhibits a linear relationship with elastic recovery up to a certain value; however, any increase beyond that point does not significantly alter the quantity of spring-back. We believe that the elastic recovery phenomenon in sheet metal U-bending can be mitigated by effectively integrating process factors, notably the three principal parameters listed, despite this work being conducted with a specific model process.

REFRENCES

[1] El-Bana R, Fouda N, Samuel M. Experimental and Numerical Prediction of Spring back in U-bending Process. MEJ-Mansoura Engineering Journal. 2020 May 7;40(1):60-71.

[2] Talebi-Ghadikolaee H, Naeini HM, Ghadikolaee ET, Mirnia MJ. Predictive modeling of damage evolution and ductile fracture in bending process. Materials Today Communications. 2022 Jun 1; 31:103543.

[3] Chen, T. C., Chen, S. X., & Wang, C. C. (2022). Punch motion curve in the extrusion–drawing process to obtain circular cups. *Machines*, *10*(8), 638.

[4] Spathopoulos SC, Stavroulakis GE. Springback prediction in sheet metal forming, based on finite element analysis and artificial neural network approach. Applied Mechanics. 2020 Apr 6;1(2):97-110...

[5] S Bhujangrao, T., Veiga, F., Penalva, M., Costas, A., & Ruiz, C. (2022). Three-dimensional finite element modelling of sheet metal forming for the manufacture of pipe components: Symmetry considerations. *Symmetry*, *14*(2), 228.

[6] Li, X., & Hu, S. (2021, November). Research Progress of Springback in Multi-Point Forming of Sheet Metal. In *Journal of Physics: Conference Series* (Vol. 2101, No. 1, p. 012006). IOP Publishing.

[7] Basirat, R., & Hamidi, J. K. (2020). Numerical Modeling of a Punch Penetration Test Using the Discrete Element Method. *Slovak Journal of Civil Engineering*, *28*(2), 1-7.

[8] Zhang, S. Q., & Zhang, S. Q. (2021). Finite Element Formulations. Nonlinear Analysis of Thin-Walled Smart Structures, 77-99..

[9] Kulikovskii, A. G., & Sveshnikova, E. I. (2021). *Nonlinear waves in elastic media*. CRC Press.

[10] Bian NH, Li G. Lagrangian Perspectives on the Small-scale Structure of Alfvénic Turbulence and Stochastic Models for the Dispersion of Fluid Particles and Magnetic Field Lines in the Solar Wind. The Astrophysical Journal Supplement Series. 2024 Jul 9; 273(1):15.

[11] Sarath S, Paul PS. Application of smart fluid to control vibration in metal cutting: a review. World Journal of Engineering. 2021 May 28;18(3):458-79.

[12] Chisena RS, Chen L, Shih AJ. Finite element composite simplification modeling and design of the material extrusion wave infill for thin-walled structures. International Journal of Mechanical Sciences. 2021 Apr 15; 196:106276.

[13] Hou Y, Myung D, Park JK, Min J, Lee HR, El-Aty AA, Lee MG. A review of characterization and modelling approaches for sheet metal forming of lightweight metallic materials. Materials. 2023 Jan 15;16(2):836.

[10] Stickle, M. M., Molinos, M., Navas, P., Yagüe, Á., Manzanal, D., Moussavi, S., & Pastor, M. (2022). A component-free Lagrangian finite element formulation for large strain elastodynamics. *Computational Mechanics*, 1-22.

[11] Eldeeb, A. M., Shabana, Y. M., & Elsawaf, A. (2021). Thermo-elastoplastic behavior of a rotating sandwich disc made of temperature-dependent functionally graded materials. *Journal of Sandwich Structures & Materials*, *23*(5), 1761-1783.

 [12] Saadatfar, M., Babazadeh, M. A., & Babaelahi, M. (2024). Creep analysis in a rotating variable thickness functionally graded disc with convection heat transfer and heat source. *Mechanics of Time-Dependent Materials*, *28*(1), 19-41.

[13] J.R. Cho, H.S. Jeong, Parametric investigation on the surface defect occurrence in CONFORM process, Mater. Process. Technol. 104 (2000) 236–243.

[14] Areias P, de Melo FQ, Sikta JN. Anisotropic hyperelastic/plastic behavior on stress-constrained thin structures by iterating on the elastic Cauchy–Green tensor. Thin-Walled Structures. 2022 Jan 1; 170:108512.

[15] Liu C. Nonuniform stress field determination based on deformation measurement. Journal of Applied Mechanics. 2021 Jul 1;88(7):071005.

[16] Anderson D, Tannehill JC, Pletcher RH, Munipalli R, Shankar V. Computational fluid mechanics and heat transfer. CRC press; 2020 Dec 17.

[17] Kumar A, Rath S, Kumar M. Simulation of plate rolling process using finite element method. Materials Today: Proceedings. 2021 Jan 1; 42:650-9.